



Title	Transition-Metal Catalysis with Hollow-Shaped Triethynylphosphine Ligands
Author(s)	Iwai, Tomohiro; Sawamura, Masaya
Citation	Bulletin of the Chemical Society of Japan, 87(11), 1147-1160 https://doi.org/10.1246/bcsj.20140186
Issue Date	2014-11-15
Doc URL	http://hdl.handle.net/2115/57758
Type	article (author version)
File Information	BCSJ_87_1147-.pdf



[Instructions for use](#)

Transition Metal Catalysis with Hollow-shaped Triethynylphosphine Ligands

Tomohiro Iwai and Masaya Sawamura*

Department of Chemistry, Faculty of Science, Hokkaido University, Sapporo 060-0810, Japan

Received ### ##, ###; E-mail: sawamura@sci.hokudai.ac.jp

Triethynylphosphines with bulky end caps such as triarylsilyl and triarylmethyl groups at alkyne termini have a novel molecular shape presenting a deep and large-scale metal-binding cavity. The hollow-shaped triethynylphosphines functioned as effective ligands in the rhodium-catalyzed hydrosilylation of ketones with a triorganosilanes due to the preferential formation of a mono-P-ligated rhodium species. Furthermore, the phosphines displayed remarkable rate enhancement in the gold(I)-catalyzed alkyne cyclization constructing six- to eight-membered ring compounds. It is proposed that the cavity in the ligand forces a nucleophilic center of the acetylenic compounds close to the gold-bound alkyne, making ring-closing anti attack feasible.

Introduction

Tertiary phosphines are the most versatile class of compounds as ligands of transition metal complexes.¹ In our investigation on the molecular design of new ligands, the intriguing structure of triethynylphosphines [P(C≡CR)₃] attracted our deep interest.² Owing to the linearity of the sp-hybridized carbons, it possesses a rigid tripod framework with the minimum steric demand around the phosphorus center. The entire structure can be modified through the substituents at the alkyne termini without affecting the steric environment in proximity to the phosphorus center.

In using phosphinoalkynes as a supporting ligand for transition metal catalysis, their bimodal coordination properties would be a potential problem.^{3,4} While the coordination at the P center is usually dominant, multi-metal complexes involving alkyne–metal interactions have also been reported. In addition, the alkyne site possesses various reactivities.⁵ Therefore, no catalytic application of phosphinoalkyne had been reported until we reported the alkyne cyclization catalyzed by gold(I) complexes coordinated with triethynylphosphine ligands (**L1** and **L2**).⁶ In this study, we reasoned that a bulky substituent at the alkyne termini could protect the C–C triple bond of the ligand from attack by the metal to facilitate the η^1 -coordination at the P center. We further conceived that a triethynylphosphine triply substituted with the bulky group would serve as an interesting structure motif for a supporting ligand in homogeneous catalysis, giving a deep and large cavity above the phosphine lone pair.

This account overviews our studies on the synthesis, properties, and catalytic uses of a new class of tertiary phosphine ligands, triethynylphosphines end-capped with silicon (**L1** and **L2**) and carbon (**L3** and **L4**) atoms trisubstituted with *m,m*-disubstituted (or *m,m,p*-trisubstituted) aromatic rings (Figure 1), which contain the phosphinoalkyne structure motif. The most salient feature of these phosphines is the large, deep metal-binding cavity. The hollow-shaped phosphines displayed remarkable rate enhancement in the various transition metal catalyzed reactions such as the rhodium-catalyzed hydrosilylation of ketones and the gold(I)-catalyzed alkyne cyclizations.

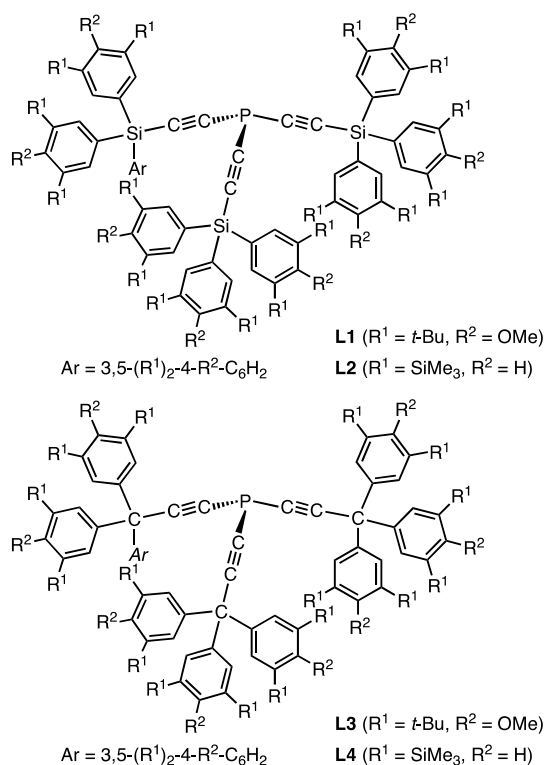
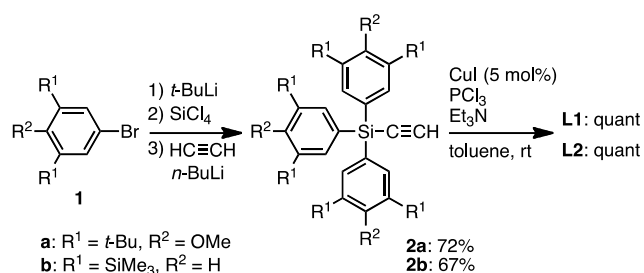


Figure 1. Triethynylphosphines bearing bulky end-caps with substituted silicon (**L1** and **L2**) and carbon (**L3** and **L4**) atoms.

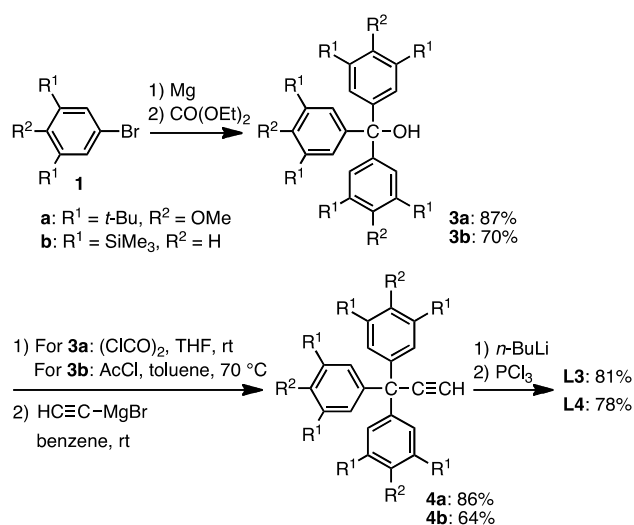
Ligand Synthesis

The synthesis of tris(triarylsilylethynyl)phosphines (**L1** and **L2**)^{6,7} and tris(triarylmethylethynyl)phosphines (**L3** and **L4**)⁸ is straightforward. For the synthesis of **L1**, SiCl₄ was first reacted with 3 eq of the aryllithium prepared from bromoarene **1a** and *t*-BuLi, and then with excess ethynyllithium to give triarylsilylacetylene **2a** in 72% yield based on **1a** (Scheme 1).

The threefold P–C coupling between PCl_3 and the silylacetylene **2a** under the copper-catalyzed conditions with excess Et_3N as a base afforded **L1** in a quantitative yield.⁹ The analogous phosphine ligand **L2** with 3,5-bis(trimethylsilyl)phenyl substituents was obtainable in a similar manner from bromoarene **1b**. The preparation of the ligand **L3** with carbon pivots is shown in Scheme 2. The reaction of diethyl carbonate with 3.3 eq of the Grignard reagent prepared from **1a**, gave triarylmethanol **3a**. The alcohol **3a** was converted to terminal alkyne **4a** by treatment of oxalyl chloride followed by ethynylmagnesium bromide. The reaction between PCl_3 and lithium acetylide prepared from **4a** and *n*-BuLi gave **L3** in high yield. The analogous ligand **L4** was synthesized from **1b** in a similar manner.



Scheme 1. Synthesis of **L1** and **L2**.



Scheme 2. Synthesis of **L3** and **L4**.

Ligand Properties

The hollow-shaped triethynylphosphines **L1–L4** are stable against air oxidation not only in crystal form but also in solution. Owing to the low-laying sp-hybridized carbon atomic orbitals associated with the C–P bond, alkynylphosphines are generally poor electron donor and hence show relatively high stability against air-oxidation at the phosphorus center when compared with alkylphosphines and

even with arylphosphines. For example, no detectable oxidation occurred upon exposure of the crystalline **L1** and **L2** for a week. Solutions of **L1** in C_6D_6 and CDCl_3 that were prepared without exclusion of air underwent almost no oxidation after standing for 72 h: ^{31}P NMR indicated only traces of signals at -60.3 and -57.3 ppm, respectively. Similar experience with **L3** also showed almost no oxidation of the phosphorous center.

Triethynylphosphines are considered to have a lower basicity than ordinary tertiary phosphines (PR_3 , R = alkyl or aryl) owing to the high electronegativity of the sp-hybridized carbon atoms bonded to the phosphorous atom. DFT calculations (B3LYP/6-31G(d,p)) indicated that the P-donor ability of the simplest trialkynylphosphine $\text{P}(\text{C}\equiv\text{CH})_3$ is comparable with that of the triphenylphosphite $\text{P}(\text{OPh})_3$. According to the ^{31}P NMR spectra of the hollow-shaped triethynylphosphines (**L1**, -85.2 ppm; **L2**, -83.0 ppm; **L3**, -86.5 ppm; **L4**, -81.8 ppm, in CDCl_3), substitution of the Si with C atom caused only marginal differences in the electronic properties (electron density and hybridization) of the central P atom.

The hollow-shaped molecular structure of **L2** was established by single-crystal X-ray diffraction analysis. An ORTEP drawing is shown in Figure 2.¹⁰ The molecule adopts a nearly C_3 symmetric conformation. Three of the eighteen terminal Me_3Si groups overhang the C–C triple bond moieties, projecting toward the phosphorus lone pair. The Me_3Si group exert a considerable steric demand on the phosphine with respect to the concept of cone angle, but leave a room large enough to accommodate a transition metal fragment that bears common ligands above the phosphorus lone pair region. Furthermore, the molecular model predicted that the cavity should be slightly deeper in the triarylmethyl-type ligands (**L3** and **L4**) than in the triarylsilyl derivatives (**L1** and **L2**), and the upper opening of the cavity should be smaller in **L1** and **L2**, than in **L3** and **L4** (Figure 3).

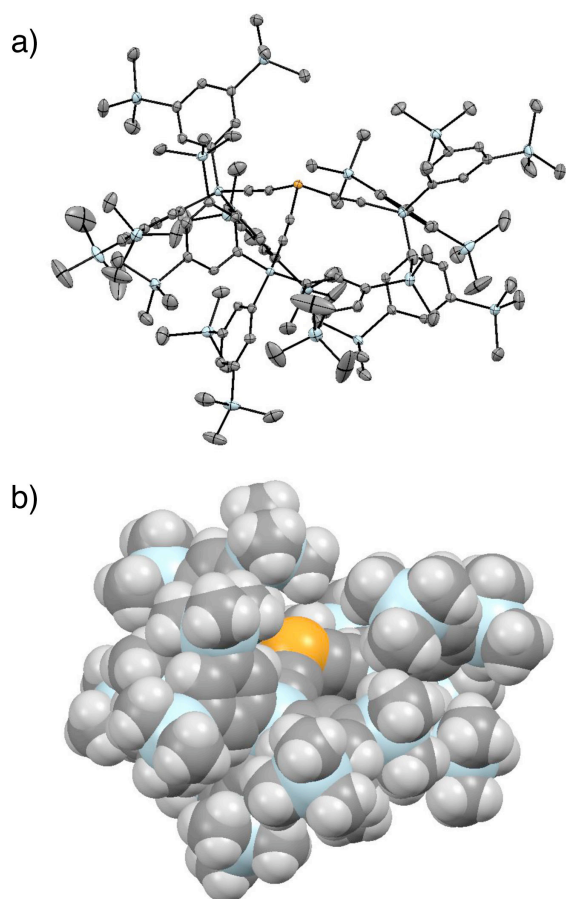


Figure 2. a) An ORTEP drawing for the molecular structure of **L2** as determined by X-ray single-crystal diffraction; hydrogen atoms and a hexane molecule are omitted for clarity. b) A space-filling representation.

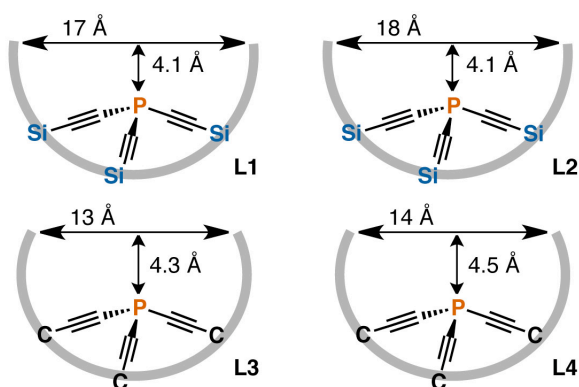


Figure 3. Estimated structural parameters of **L1–L4**.

Rhodium Complexes

The triethynylphosphines **L1–L4** favored to form mono-P-ligated metal complexes due to the steric bulkiness at the periphery of the phosphines. Specifically, the reaction of $[\text{RhCl}(\text{cod})]_2$ with **L1** in a Rh:P ratio of ca. 1:1.1 in C_6D_6 at rt

resulted in the formation of a mono-P-ligated complex $[\text{RhCl}(\text{cod})(\text{L1})]$.⁷ The ^{31}P NMR spectra showed a doublet with a Rh–P coupling at $\delta -47.8$ ($^1J_{\text{P-Rh}} = 167$ Hz), indicating η^1 -coordination of **L1** at the phosphorus atom. It should be noted that the reaction produced neither bis-P-ligated nor tris-P-ligated mononuclear complexes. This is what expected from the results of molecular modeling examinations that the ligands are too bulky to form multi-P-ligated complexes.

The molecular structure of $[\text{RhCl}(\text{cod})(\text{L2})]$ was determined by single crystal X-ray diffraction analysis.¹⁰ An ORTEP drawing for the molecular structure is given in Figure 4. The $\text{RhCl}(\text{cod})$ fragment is fully accommodated by the cavity created by the phosphine ligand. There still exists a considerable space between the metal fragment and the interior surface of the ligand cavity, implying that the complex may be susceptible to the access of a molecule to undergo a further metal-centered reaction.

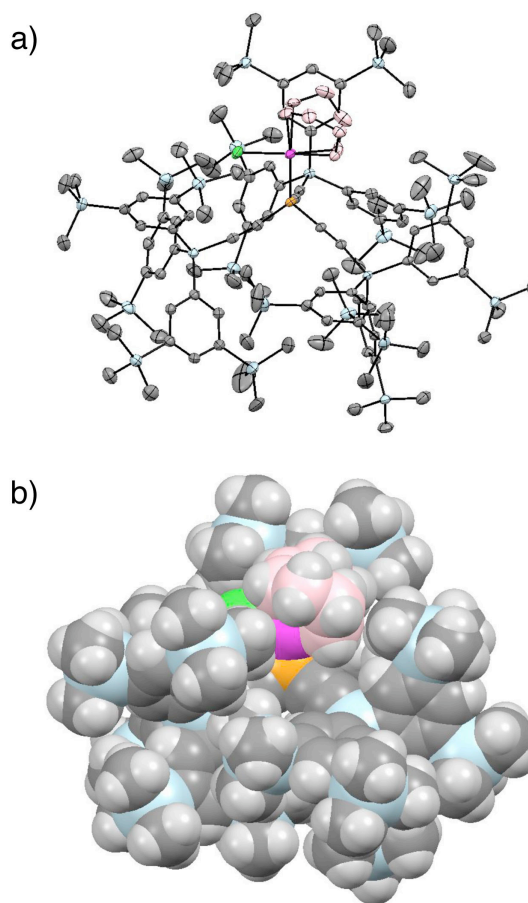


Figure 4. a) An ORTEP drawing for the molecular structure of $[\text{RhCl}(\text{cod})(\text{L2})]$ as determined by X-ray single-crystal diffraction; hydrogen atoms are omitted for clarity. b) A space-filling representation.

Rhodium-Catalyzed Hydrosilylation of Ketones

Tsuji and co-workers reported that bowl-shaped phosphine ligands,¹¹ which bear *m*-terphenyl-based P substituents, accelerated markedly the rhodium-catalyzed hydrosilylation of ketones compared to the effects of ordinary phosphine ligands such as PPh₃ and P(*t*-Bu)₃, and proposed that a mono-P-ligated rhodium species was responsible for the acceleration.¹² We also reported the similar ligand-acceleration effect by the bulky isocyanides¹³ and silica-supported caged trialkylphosphine Silica-SMAP.¹⁴ Thus, the mono-P-ligation of the bulky triethynylphosphines led us to examine the effect of **L1** and **L2** in the Rh-catalyzed hydrosilylation.⁷

Reaction of cyclohexanone (1 mmol) and PhMe₂SiH (1.2 mmol) was carried out in benzene (1 mL) at room temperature in the presence of 0.5 mol% amount of [RhCl(cod)]₂ and 1–2 mol% amount of a phosphine (Rh/P 1:1 or 1:2, Table 1). With a P/Rh ratio of 1:1, the reaction with *t*-Bu-substituted ligand **L1** was fastest, completing within 2 h (entry 1). The reaction with **L2** was slightly slower than that with **L1** (entry 2). The results with other triethynylphosphines (**L5–L8**) indicated that the reaction further slowed down as the bulkiness of the alkyne end-capping groups of the triethynylphosphines become smaller (entry 3–6). Conventional triarylphosphine PPh₃ showed no accelerating effect when compared with the result in the absence of added phosphine ligand (entries 7 and 8).

The increase of P/Rh ratio to 2:1 caused only small decrease in the rate of conversion, using **L1** and **L2**, while those with **L5**, **L7** and **L8** resulted in almost complete loss of the catalytic activity (Table 1, entries 1–6). The catalyst deactivation by the second equivalency of the phosphine ligands (**L5**, **L7** and **L8**) must be due to bis- or tris-P-ligation of the phosphine ligands to the rhodium center. These results strongly suggest that a mono-P-ligated rhodium is a catalytically active species and is favored with **L1** and **L2**.

Table 1. Ligand Effects in Rh-catalyzed Hydrosilylation of Cyclohexanone with PhMe₂SiH.

[RhCl(cod)]₂ (Rh: 1 mol%)
ligand (P: 1–2 mol%)
benzene (1 mL)
25 °C, 2 h

entry	ligand	yield (% GC)	
		P/Rh 1:1	P/Rh 2:1
1	L1	96	91
2	L2	88	77
3	P(C≡CSiPh ₃) ₃ (L5)	75 ^a	1
4	P(C≡CSi(<i>i</i> -Pr) ₃) ₃ (L6)	36	79
5	P(C≡CSiMe ₃) ₃ (L7)	19	2
6	P(C≡CPh) ₃ (L8)	2	1
7	PPh ₃	8 ^a	–
8	none	4 ^a	–

^aReaction time is 3 h.

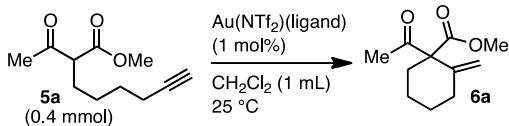
Gold(I)-Catalyzed Alkyne Cyclizations

Electrophilic activation of an alkyne by the coordination of a π -Lewis acidic metal cation induces the attack of a nucleophile that locates at an appropriate position within the molecule. For such alkyne cyclizations, gold is one of the most active catalysts among various metal ions, and gold–phosphine complexes have been applied to alkyne cyclizations of various types.¹⁵ The ring-forming gold catalyzed reactions, however, suffer from at least two serious problems. First, they are limited to the cases where cyclization is entropically quite favorable such as five-membered ring formations. Second, the cyclizations of internal alkynes are often hampered by steric repulsion between the terminal substituent and nucleophiles at the carbon–carbon and carbon–heteroatom bond forming steps.

We conceived that the holey catalytic environments created in triethynylphosphines with bulky end caps at alkyne termini (**L1–L4**) might be advantageous for cyclization reactions because the gold-bound alkyne substrate should adopt a bent conformation to fit in the cavity of the semihollow ligand, resulting in entropy-based rate enhancement of the reaction between the nucleophile and the ionized alkyne moiety due to close proximity between the two reaction centers. Based on this consideration, we decided to apply the triethynylphosphine ligands to gold(I)-catalyzed alkyne cyclization reactions.

Conia-Ene Reaction of Terminal Alkynes. The triethynylphosphine **L1** showed a marked advantage over conventional phosphine ligands when applied to the gold(I)-catalyzed 6-*exo-dig* cyclization of acetylenic keto esters.⁶ It should be noted that the gold(I)-catalyzed 6-*exo-dig* cyclization of simple acetylenic keto esters leading to monocyclic methylenecyclohexane derivatives had not been described in the literature until we reported the following results.^{16–18} Specifically, treatment of **5a** with a CH₂Cl₂ solution containing 1 mol% cationic gold(I) complex [Au(NTf₂)(**L1**)] (Tf = SO₂CF₃), which was prepared from the neutral complex [AuCl(**L1**)] and AgNTf₂,^{17c} resulted in smooth conversion at room temperature, the reaction being completed within 1.5 h to afford **6a** in quantitative yield (Table 2, entry 1). In contrast, there was almost no reaction with the corresponding PPh₃ complex (entry 2). Bulky, biphenyl-based phosphines such as SPhos¹⁹ and XPhos,¹⁹ which were reported to be exquisite ligands in the gold-catalyzed alkyne cyclizations, failed to activate the gold catalyst in promotion of the present reaction (entries 3 and 4). The complexes formed with the P(OPh)₃ and P(O-2,4-(*t*-Bu)₂-C₆H₃)₃ ligands, whose donor powers are estimated to be comparable with the triethynylphosphines, catalyzed the cyclization with much lower efficiency (entries 5 and 6). The existence of a bulky substituent in the triarylphosphite had only a little influence on the activity of the gold catalyst.

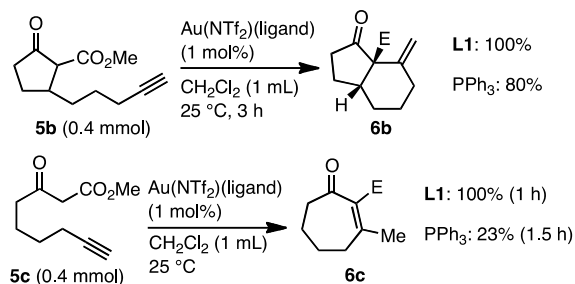
Table 2. Ligand Effects in Gold(I)-Catalyzed Conia-Ene Reaction of **5a**.



entry	ligand	time (h)	yield (%), ¹ H NMR
1	L1	1.5	100
2	PPh ₃	1.5	3
3	SPhos	1.5	<1
4	XPhos	1.5	<1
5	P(OPh) ₃	6	21
6	P(O-2,4-(<i>t</i> -Bu) ₂ -C ₆ H ₃) ₃	6	28
7	L2	5	70
8	P(C≡CSiPh ₃) ₃ (L5)	2.5	4
9	P(C≡CSi(<i>i</i> -Pr) ₃) ₃ (L6)	1.5	13

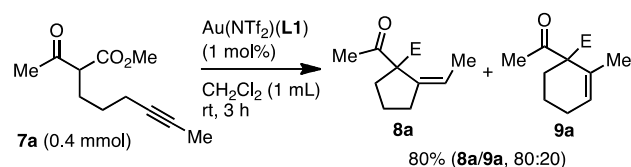
Comparison of triethynylphosphines (**L1**, **L2**, **L5**, **L6**) bearing silicon end caps with varying steric demands and shapes indicated that a ligand steric factor is crucial for promotion of the cyclization. The gold complex Au-**L2** with showed apparently lower catalytic activity than Au-**L1**, achieving only 70% conversion after 5 h (Table 2, entry 7). The ligand with SiPh₃ (**L5**) and Si(*i*-Pr)₃ (**L6**) end caps, whose steric demands are fairly large in the vicinity of the ligand alkyne moiety but is too small to reach to the reaction site, were far less effective (entries 8 and 9). These results clearly indicate that the *meta* substituents (*t*-Bu and Me₃Si) of **L1** and **L2** play a critical role in promotion of cyclization.

The gold complex Au-**L1** (1 mol%) was applied to the cyclization of other acetylenic substrates, and was compared with the PPh₃ complex in terms of catalytic activity (Scheme 3). In accordance with our assumption in the ligand design, the catalytic benefit of **L1** was significantly diminished in the reaction of cyclic substrate **5b**, which is programmed for cyclization via insertion of a ring between the alkyne and keto ester moieties. The superior performance of **L1** over PPh₃ recovered reasonably in the 7-*exo-dig* cyclization of linear acetylenic ketoester **5c** that afforded a seven-membered ring compounds as a mixture of **6c** and its enol form (65:35) after base-catalyzed isomerization.



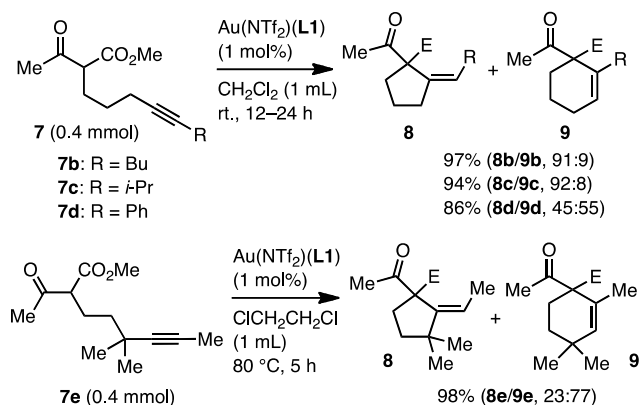
Scheme 3. Conia-Ene Reactions of **5b** and **5c** (E = CO₂Me).

Conia-Ene Reaction of Nonterminal Alkynes. Generally, internal alkynes are poor substrates for gold-catalyzed cyclizations. The low reactivity of this type of substrates should be due to steric repulsions caused by the terminal substituent. Benefits of using the hollow-shaped phosphine **L1** was demonstrated even in the challenge toward this type of problems in gold catalysis. In fact, the gold(I) complex with **L1** catalyzed the cyclizations of nonterminal alkynic β-keto esters that afford the sterically congested five- and six-membered ring compounds.²⁰ Treatment of **7a** with a CH₂Cl₂ solution of [Au(NTf₂)(**L1**)] (1 mol%) resulted in smooth conversion at room temperature; the reaction completed within 3 h to afford 5-*exo-dig* and 6-*endo-dig* cyclization products **8a** and **9a** in a good combined yield, with preference to the former (80:20), which seems to be sterically more congested and hence energetically less favorable but entropically more favorable than the latter (Scheme 4). No *E*-isomer of *exo*-alkene **8a** was formed, suggesting *anti*-stereochemistry of a nucleophilic attack to a gold-alkyne π-complex. In contrast, there were only low conversions with the corresponding PPh₃ and P(OPh)₃ complexes even when the reaction time was prolonged to 24 h (<13% conv. of **7a**).



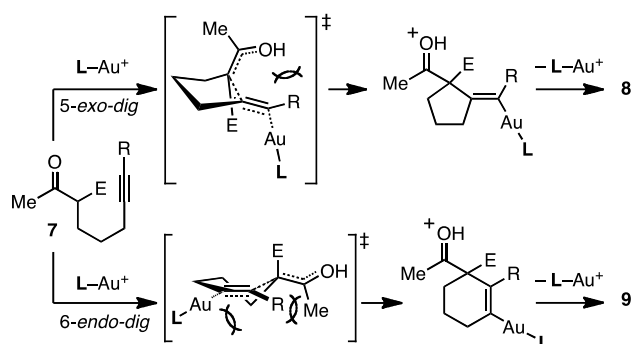
Scheme 4. Conia-Ene Reaction of Internal Alkene **7a** (E = CO₂Me).

With the internal alkynes (**7b–7d**) bearing bulkier terminal substituents such as Bu, *i*-Pr and Ph groups, the reaction with the Au-**L1** catalyst proceeded smoothly, and afforded the corresponding five- and six-membered ring compounds (**8b–8d/9b–9d**) in high combined yields (Scheme 5). The reaction of the acyclic alkyne (**7e**) bearing a quaternary carbon center at the internal α-position proceeded at 80 °C in 1,2-dichloroethane to give a mixture of 5-*exo-dig* (**8e**) and 6-*endo-dig* (**9e**) cyclization products in favor of the 6-*endo* isomer.



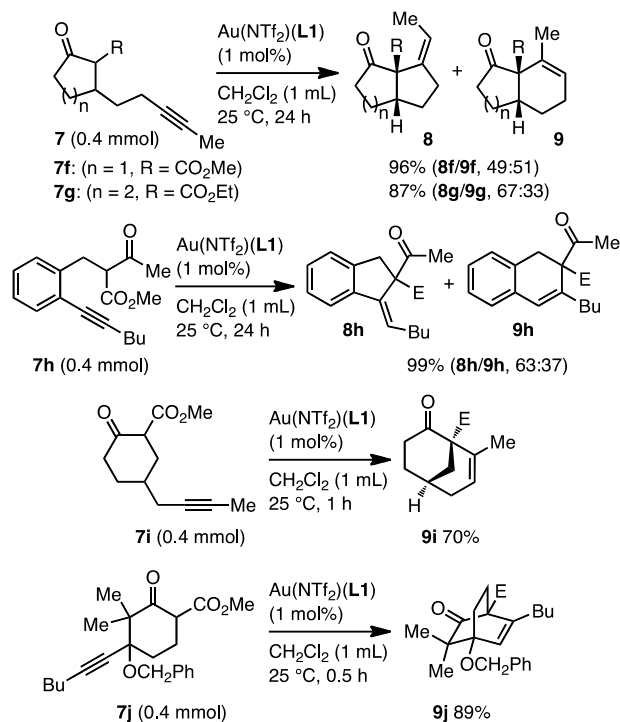
Scheme 5. Conia-Ene Reactions of **7b–7e** (E = CO₂Me).

The effect of the terminal substituent of **7** on the 5-*exo*/6-*endo* selectivity may give an insight into the mechanism of the gold-catalyzed Conia-ene reaction. As the terminal alkyl substituents became bulkier (Me < Bu < *i*-Pr), the selectivity for 5-*exo* product **8** increased: 80%, 91% and 92% with **L1** (Schemes 4 and 5). In the proposed C–C bond forming transition states (Scheme 6), the terminal substituent should encounter steric repulsions not only with the incoming nucleophile but also with the Au–L moiety. The former should be larger in the 5-*exo*-transition state, while the latter in the 6-*endo*-transition state. Accordingly, the increase of the *exo* selectivity upon the increase of the size of the terminal substituent R is likely due to the steric repulsion between R and the Au–L moiety. In the reaction of **7e** (Scheme 5), the Au–L fragment encounters more steric repulsion with the geminally substituted inner substituent than with the terminal Me substituent.



Scheme 6. Proposed Mechanism for the Reaction of **7** (E = CO₂Me).

The Au–**L1** system was further found to allow the Conia-ene reaction of various internal alkynes, to give the corresponding cyclic keto esters (Scheme 7). When [Au(NTf₂)](**L1**) (1 mol%) was employed, the 5-*exo*/6-*endo* annulation of an alkyne pendant onto a cyclopentanone **7f** and a cyclohexanone **7g** completed within 24 h to afford **8f/9f** (49:51) and **8g/9g** (67:33), respectively, in high yields and in complete diastereoselectivity. The Au–**L1** catalyst achieved quantitative conversion for **7h** bearing aromatic ring between an alkyne and a nucleophile. Notably, the reaction of **7i** proceeded with complete regioselectivity to afford bicyclo[3.3.1]nonenone **9i**. Additionally, similar results were obtained in the reaction of **7j** which provided highly substituted bicyclo[2.2.2]octenone derivative **9j**.



Scheme 7. Conia-Ene Reactions of **7f–7j** (E = CO₂Me).

Enyne Cycloisomerization. The hollow-shaped triethynylphosphine (**L1**) could assist gold(I)-catalyzed cycloisomerization (1 mol% Au) of 1,7-enynes more successfully than PPh₃.^{6,21,22} Thus, the reaction of **10a** (0.02 M), which bears a malonate group at the bishomopropargyl position, with **L1** completed in 20 min to afford **11a** in 75% yield, while the reaction with PPh₃ exerted only 9% conv. at 20 min (Table 3, entries 1 and 2). The reaction of **10b** (0.1 M) bearing a malonate group at the homopropargyl position proceeded very fast irrespective of using either **L1** or PPh₃, being completed in 10 min to afford **11b** (as an isomer mixture) in high yields (entries 3 and 4). Perhaps this means that Thorpe-Ingold effect worked more efficiently for **10b** than for **10a**, and that the steric effect of the hollow-shaped ligand **L1** did not operate efficiently in the reaction of the programmed substrate (**10b**). Eliminating the Thorpe-Ingold effect through the replacement of the malonate linker of **10b** with an etheral one (**10c**) resulted again in the recovery of the superiority of **L1** over PPh₃ (entries 5 and 6).

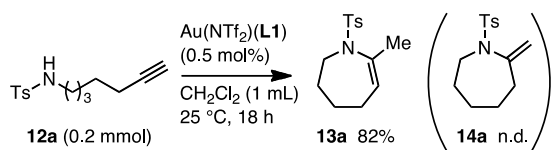
Table 3. Gold(I)-Catalyzed Cycloisomerization of 1,7-Enyne **10**.^a

entry	alkyne 10	product 11	ligand	time (min)	yield (%) ^b
1			L1	20	75
2			PPh ₃	20	9 ^c
3			L1	10	94
4			PPh ₃	10	90
5			L1	15	75
6			PPh ₃	15	9 ^c

^a**10** (E = CO₂Me, 0.4 mmol), [Au(NTf₂)(**L1**)] (1 mol%), CH₂Cl₂ (20 mL for entries 1, 2, 5 and 6; 4 mL for entries 3 and 4), rt.
^bIsolated yield. ^cConversion of **10** determined by ¹H NMR.

Intramolecular Hydroamination. Nitrogen-containing heterocyclic seven-membered rings are found in many biologically active natural products and pharmaceuticals.²³ Among numbers of approaches for constructing *N*-heterocyclic compounds, metal-catalyzed intramolecular hydroamination of unactivated C–C multiple bonds is particularly straightforward and efficient.²⁴ Despite extensive studies on the gold-catalyzed intramolecular hydroamination of alkynes, seven-membered ring formation is rare and limited to the cases where the substrate is preorganized for cyclization: the substrates must have geminal disubstitution or ring fusion within a linker chain connecting the attacking nitrogen atom and the alkyne moiety.

The use of **L1** as a ligand in the gold catalyzed intramolecular hydroamination of alkyne sulfonamides would enable the construction of nitrogen-containing heterocyclic seven-membered rings such as tetrahydroazepins through a *7-exo-dig* cyclization mode.²⁵ Thus, the cationic gold complex [Au(NTf₂)(**L1**)] (0.5 mol%) catalyzed the cyclization of *N*-(6-heptyn-1-yl)-*p*-toluenesulfonamide **12a** (0.2 mmol) efficiently in CH₂Cl₂ (1 mL) at 25 °C (100% conv. of **12a**) to afford 4,5,6,7-tetrahydroazepine derivative **13a** with 18 h reaction time in 82% isolated yield (Scheme 8). Interestingly, an exomethylene-type cyclic product **14a**, which is a possible product of the *7-exo-dig* cyclization, was not observed at all. Other ligands such as P(OPh)₃, XPhos and IPr²⁶ were less effective than **L1** under otherwise identical conditions (<41% yield of **13a**).

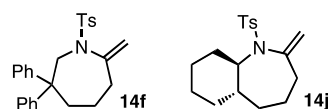
**Scheme 8.** Intramolecular Hydroamination of **12a**.

A substrate scope of the alkyne *N*-tosylsulfonamides bearing linear or cyclic linkers with the [Au(NTf₂)(**L1**)] catalyst system is shown in Table 4. The introduction of the substituents at the α- or β-positions relative to the alkyne moiety caused a significant decrease in the reactivity, but the cyclization of the substituted alkyne sulfonamide **12b–12g** proceeded smoothly with 2.5–5 mol% catalyst loading at 80 °C into full substrate conversion (entries 1–6). For the construction of bicyclic frameworks, the cyclization of *o*-alkynyl benzylsulfonamide **12h** and benzamide **12i** gave benzazepine **13h** and ε-caprolactam within an exomethylene structure **14i**, respectively, in high yields (entries 7 and 8). Alkyne sulfonamide **12j** with a cyclohexane-fused linker also participated in the cyclization to form azabicyclo[5.4.0]decene **13j** in 76% yield along with a small amount of exomethylene isomer **14j** (**13j/14j** 98:2, entry 9).

Table 4. Gold(I)-Catalyzed Cyclization of Alkyne Sulfonamides **12**.^a

entry	alkyne 12	product 13	time (h)	yield (%) ^b
1			8	99
2			12	88
3			12	71
4			4	77
5			4	69 ^c
6			12	66
7			3	86
8			3	97
9			17	76 ^d

^a**12** (0.1 mmol), [Au(NTf₂)(**L1**)] (2.5 mol% for entries 1, 7 and 9; 5 mol% for entries 2–6 and 8), ClCH₂CH₂Cl (1 mL), 80 °C.
^bIsolated yield. ^c**13f/14f** 92:8. ^d**13j/14j** 98:2.

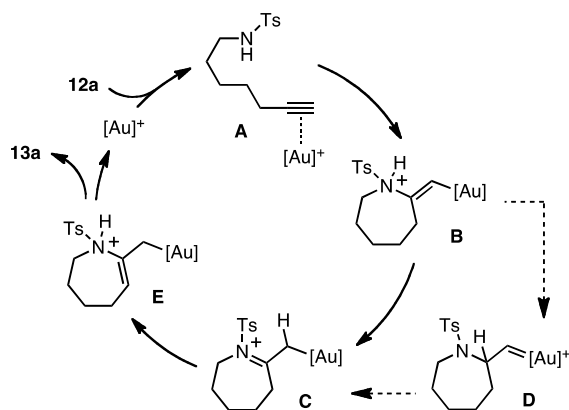


The triethynylphosphine ligand **L1** was also evaluated for the eight-membered ring formation of sulfonamide **15**, which is much more challenging than the seven-membered ring formation of **12** (Scheme 9). The reaction required 5 mol% catalyst loading under heating conditions (80 °C) in 1,2-dichloroethane solvent for a reasonable conversion rate to afford an eight-membered ring azocine derivative **16** in 15% isolated yield along with significant amounts of unidentified oligomeric side products.



Scheme 9. 8-Exo-dig Cyclization of **15**.

A possible reaction pathway from **12a** to **13a** is illustrated in Scheme 10. First, the cationic gold center coordinates with **12a** to form gold–alkyne complex **A**. Intramolecular nucleophilic attack of the nitrogen atom affords a 7-*exo-dig* cyclization product (**B**) with an exocyclic C–C double bond. The protonated *N*-sulfonylenamide **B** tautomerizes to iminium ion **C** through 1,3-proton shift or through an alternative pathway via a gold(I)-carben intermediate (**D**). Then, re-tautomerization affords protonated *N*-sulfonylenamide **E** with an endocyclic C–C double bond. Finally, protodemetalation of **E** give the *N*-sulfonylenamide **13a**, which is thermodynamically more stable than **14a**.

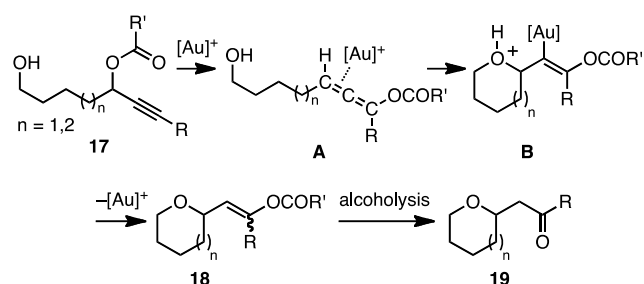


Scheme 10. Possible Pathway from **12a** to **13a**.

Cyclization of Hydroxy-Tethered Propargylic Esters.

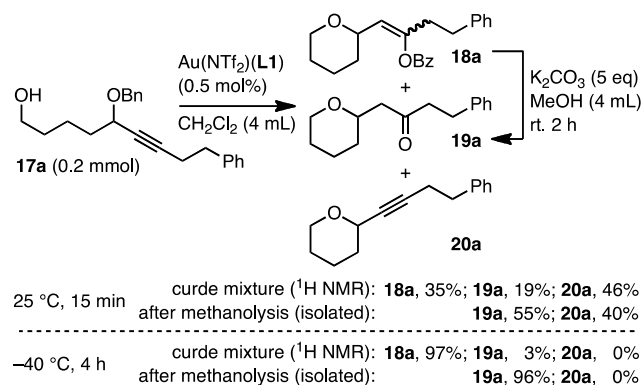
Formation of six- and seven-membered ring ethers from hydroxy-tethered propargylic esters was efficiently catalyzed by a cationic gold(I) complex with a hollow-shaped triethynylphosphine ligand (**L1**).²⁷ This reaction likely proceeds via gold-catalyzed intramolecular hydroalkoxylation allenyl carboxylate **A**, which is formed through gold-catalyzed [3,3]sigmatropic rearrangement of propargylic ester **17**, as

described by Brabander and co-workers (Scheme 11).^{28–30}



Scheme 11. Plausible Pathway for the Cyclization of Hydroxy-Tethered Propargylic Esters **17**.

The cationic gold complex [Au(NTf₂)(**L1**)] with 0.5 mol% loading in CH₂Cl₂ (4 mL) caused a rapid and complete conversion of **17a** at room temperature (<15 min) to afford a mixture of tetrahydropyran derivatives bearing alkenyl benzoate (**18a**), acylmethyl (**19a**), or alkynyl (**20a**) pendant moieties in 35%, 19%, and 46% yields, respectively (Scheme 12). After alcoholysis of the benzoyl group of **18a** (K₂CO₃/MeOH, room temperature), ketone **19a** and alkyne **20a** were isolated in 55% and 40% yields, respectively. The alkyne formation was completely inhibited by conducting the reaction at –40 °C for 4 h, and the pure ketone **19a** was obtained in 96% isolated yield after alcoholysis.



Scheme 12. Gold-Catalyzed Cyclization of **17a**.

The substrate scope of the gold catalysis with **L1** for various substitution patterns of hydroxy-tethered propargylic esters **17** is shown in Table 5. As steric demand of the substituents at the alkyne termini increased (R = Me, *n*-Bu, *i*-Bu, Cy), reaction times became longer (entries 1–4). However, the corresponding ketones **19b–19e** were obtained in high yields after alcoholysis with K₂CO₃/MeOH. The cyclization of acetal-containing substrate **17f** proceeded efficiently with a 2.5 mol% catalyst loading to give **19f** in 89% yield (entry 5). The gold catalysis with **L1** showed a good tolerance toward the sterically hindered substrates such as secondary and tertiary alcohols **17g–17i** and **17k** (entries

6–8, 10). The substrates **17j** and **17k** with alcohol-tethered tertiary propargylic esters furnished sterically congested tetrahydropyran derivatives **19j** and **19k** in useful yields along with small amounts of the alkynylated tetrahydropyrans **20**. Annulation of tetrahydropyran-tethered propargylic benzoate **17l** was smoothly converted into the 6,6-fused bicyclic diether compound **19l** with excellent diastereoselectivity (>20:1) after alcoholysis (entry 11). This strategy for heterocycle synthesis could be extended to the synthesis of *N*-heterocyclic compounds. The reaction of propargylic ester **17m**, bearing a *p*-toluenesulfonamide moiety as a nucleophile, underwent cyclization in a similar fashion with a 5 mol% catalyst loading, affording piperidine derivative **19m** in 79% yield (entry 12).

Table 5. Substrate scope of **17** Catalyzed by Au-L1 Complex.^a

entry	substrate 17	product 19	time (h)	yield (%) ^b
1	17b (R = Me)	19b (R = Me)	3	85
2	17c (R = <i>n</i> -Bu)	19c (R = <i>n</i> -Bu)	4	96
3	17d (R = <i>i</i> -Bu)	19d (R = <i>i</i> -Bu)	12	87
4	17e (R = Cy)	19e (R = Cy)	24	96
5	17f	19f	2	89
6	17g (R = Me)	19g (R = Me)	24	86 ^c
7	17h (R = <i>n</i> -Pr)	19h (R = <i>n</i> -Pr)	24	67 ^c
8	17i	19i	1.5	80
9	17j	19j	0.25	49 ^d
10	17k	19k	6	65 ^d
11	17l	19l	9	91 ^c
12	17m	19m	18	79

^a**17** (0.2 mmol), [Au(NTf₂)(**L1**)] (0.5 mol% for entries 1–4 and 6–10; 2.5 mol% for entry 5; 4 mol% for entry 11; 5 mol% for entry 12), CH₂Cl₂ (4 mL), at –40 °C. Ketone **19** was isolated after

alcoholysis with K₂CO₃ (5 eq) in MeOH (4 mL) at rt, for 2 h. ^bIsolated yield. ^cDiastereomeric mixture for **19g**, *dr* = 87/13; **19h**, *dr* = 87/13; **19l**, *dr* = >20:1. ^dAlkynylated tetrahydropyrans **20** were also obtained (entry 9, 7%; entry 10, 14%).

The gold catalyst with **L1** was also effective in the corresponding seven-membered ring formation with substrates having an additional carbon in the tether (Table 6). A simple substrate (**17n**) with a primary alcohol moiety successfully underwent seven-membered ring formation in THF (0.01 M) at room temperature for 18 h with 5 mol% catalyst loading, to give **19n** in 88% yield (entry 1). The catalyst loading can be reduced to 1 mol% without a significant decrease in the yield (entry 2). The cyclizations of tetrahydropyran-tethered substrate **17o**, cyclic tertiary alcohol substrate **17p**, and benzyl alcohol substrate **17q** proceeded to afford the corresponding seven-membered cyclic ethers **19o–19q** in good to high yields (entries 3–5).

Table 6. Seven-membered Ring Formation through Gold(I)-Catalyzed Cyclization of **17**.^a

entry	substrate 17	product 19	time (h)	yield (%) ^b
1			18	88
2	17n	19n	24	83
3			1	70
4			14	82
5			0.5	61

^a**17** (0.2 mmol), [Au(NTf₂)(**L1**)] (5 mol% for entries 1 and 3; 1 mol% for entries 2 and 4; 2 mol% for entry 5), THF (20 mL), rt. Ketones **19** was isolated after alcoholysis with K₂CO₃ (5 eq) in MeOH (4 mL) at rt for 2 h. ^bIsolated yield.

Cyclization of Acetylenic Silyl Enol Ethers: Seven-Membered Ring Formation. Gold-catalyzed intramolecular reactions of silyl enol ethers with alkynes are powerful methods for the construction of carbocyclic compounds.^{31,32} This method, however, had not been extended toward seven-membered ring formations, which seems to be difficult because of the distal location of the nucleophilic center and the alkyne moiety, with conventional catalyst systems.

The cationic gold complex bearing the hollow-shaped triethynylphosphine **L1** efficiently catalyzed the 7-*exo-dig* cyclization of acetylenic silyl enol ethers to construct a 2-methylene bicyclo[4,3,1]decane framework,³³ which is found in natural diterpenoid (+)-sanadaol (Figure 4).³⁴ Thus, the reaction of a cyclic silyl enol ether **21a** (0.1 mmol) with a catalytic amount of [Au(NTf₂)(**L1**)] (5 mol%) in the presence of *t*-BuOH (0.1 mmol) and MS4A (100 mg) in anhydrous CH₂Cl₂ (5 mL) at room temperature completed within 5 min to afford cyclization product **22a** in a quantitative yield (Scheme 13). Notably, the reaction was not accompanied by neither the direct protonation of the silyl enol ether (**21a**) to a ketone **23a** nor the double bond shift of the β,γ-unsaturated ketone (**22a**) to a conjugated enone at all, which are common side reactions of the metal-catalyzed cyclization of acetylenic silyl enol ethers. In contrast, gold complexes with other ligands such as PPh₃, P(OPh)₃, XPhos and IPr were not efficient, and did not reach full conversions of **20a** even after 3 h under otherwise identical conditions (<39% conv. of **21a**).

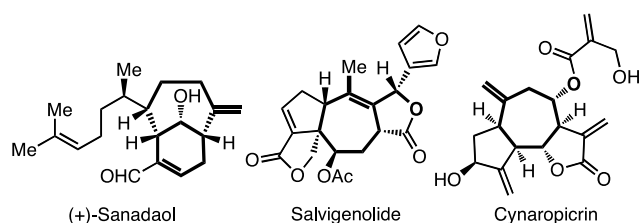
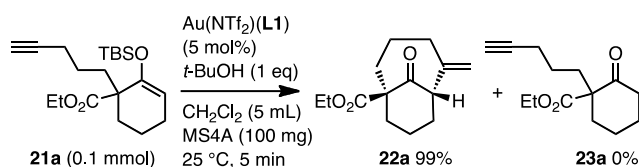


Figure 4. Natural terpenoids that possess a seven-membered ring carbocycle.



Scheme 13. Cyclization of Alkynyl Silyl Enol Ether **21a**.

The gold(I)-**L1** catalyst system was used for construction of bicyclo[4.*n*.1]alkane or bicyclo[*m*.4.1]alkane frameworks through 7-*exo-dig* cyclization with various cyclic silyl enol ethers substrates (Table 7). Triisopropylsilyl enol ether **21b** was less reactive than the TBS ether **21a**, but was rapidly (≤5 min) and quantitatively converted to **22a** at 80 °C. The reaction of the substrate bearing benzoyl group **21c** required slight heating (40 °C), and resulted in a moderate yield. Bicyclo[4.2.1]nonane (**22d**), bicyclo[4.4.1]undecane (**22e**) and bicyclo[5.4.1]dodecane (**22f**) frameworks were obtained from the corresponding cyclic silyl enol ethers **21d–21f** in excellent yields.

Table 7. Cyclization of Cyclic Alkynyl Silyl Enol Ethers **21**.^a

entry	substrate 21	product 22	temp (°C)	time	yield (%) ^b
1			80	5 min	99
2			40	2 h	74
3			25	5 min	100
4			25	5 min	96
5			25	5 min	94

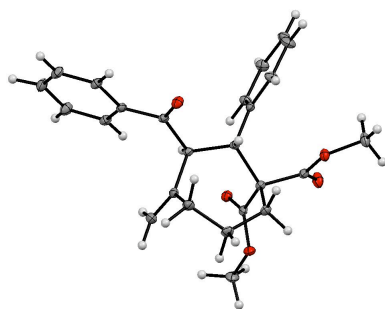
^a**21** (0.1 mmol), [Au(NTf₂)(**L1**)] (5 mol%), *t*-BuOH (0.1 mmol), MS4A (100 mg), CH₂Cl₂ (5 mL) at 25 or 40 °C, ClCH₂CH₂Cl (5 mL) at 80 °C. ^bIsolated yield.

The gold(I)-triethynylphosphine (**L1**) complex can be applied to the synthesis of monocyclic methylenecycloheptane frameworks from acyclic silyl enol ethers, which seem to be more challenging substrates due to their conformational flexibilities (Table 8). The reactions of acetylenic *Z*-configured silyl enol ethers (**21g–21i**) proceeded efficiently under relatively mild conditions (5 mol% of [Au(NTf₂)(**L1**)], 25–80 °C), to afford the corresponding seven-membered carbocycles involving an exocyclic carbonyl group (entries 1–6). The structure of **22k** was determined by X-ray crystal structure analysis (Figure 5).¹⁰ The cyclization of the *E* isomer of **21j** gave the same stereoisomer of **22j** as that of (*Z*)-**21j** (entries 4 v.s. 7), while the reaction time was prolonged to 2 h at 80 °C (entry 7). Notably, the methylenecycloheptane framework with an exocyclic carbonyl group in **22g–22i** thus prepared is reminiscent of a partial structure of diterpenoid salvigenolide (Figure 4).³⁵ The reaction of silyl enol ethers **21m** and **21n** afforded methylenecycloheptane derivatives **22m** and **22n** involving an endocyclic carbonyl group, respectively, in excellent yields (entries 8 and 9). These compounds can be structurally related to natural sesquiterpenoid cynaropicrin (Figure 4).³⁶

Table 8. Cyclization of Linear Alkynyl Silyl Enol Ethers **21**.^a

entry	substrate 21	product 22	temp (°C)	time	yield (%) ^b
1 ^c			25	5 min	93
2 ^c			25	3 h	89
3 ^c			80	5 min	93
4			80	10 min	94
5 ^c			80	24 h	51
6 ^c			40	24 h	83
7 ^c			80	2 h	85
8			25	5 min	90
9 ^d			40	5 min	93

^a**21** (E = CO₂Me, 0.1 mmol), [Au(NTf₂)(**L1**)] (5 mol%), *t*-BuOH (0.1 mmol), MS4A (100 mg), CH₂Cl₂ (5 mL) at 25 or 40 °C, ClCH₂CH₂Cl (5 mL) at 80 °C. ^bIsolated yield. ^cIsomeric mixture for **21g**, *E/Z* 14:86; **21h**, *E/Z* 13:87; **21i**, *E/Z* 10:90; **21k**, *E/Z* 4:96; **21l**, *E/Z* 19:81; (*E*)-**21j**, *E/Z* 86:14. ^d0.6 mmol scale in CH₂Cl₂ (30 mL).

**Figure 5.** An ORTEP drawing for the molecular structure of **22k**.

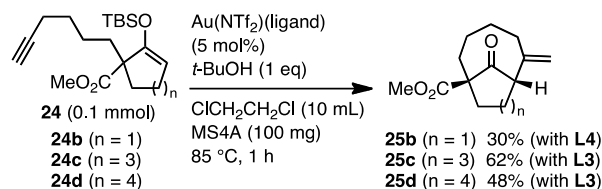
Eight-Membered Ring Formation through Cyclization of Acetylenic Silyl Enol Ethers. Next, the gold catalysts with the hollow-shaped phosphines were applied to more challenging eight-membered ring formation with substrates having additional carbon in the tether.⁸ Although the reaction of **24a** with triarylsilyl-type ligands **L1** and **L2** (5 mol% of Au, at 85 °C for 1 h) afforded methylene cyclooctane derivative **25a** in merely <12% yield (Table 9, entries 1 and 2), the triarylmethyl-type triethynylphosphine **L3** promoted this reaction efficiently, affording **25a** in 70% yield (entry 3). The other triarylmethyl-type ligand (**L4**) with Me₃Si substituents at the aromatic rings was also effective in affording **25a**, albeit with a lower yield (entry 4). The deeper and narrower cavities of **L3** and **L4** seem to be more suitable than those of **L1** and **L2** for the eight-membered-ring formation (Figure 3). With regard to the proton source, switching from *t*-BuOH to MeOH significantly improved the catalytic activity of [Au(NTf₂)(**L3**)], thus increasing the yield of **25a** to 83% with 99% conversion of **24a** (entry 5).

Table 9. Cyclization of Alkynyl Silyl Enol Ether **24a**.

entry	ligand	conv. of 24a (%) ^a	yield of 25a (%) ^a
1	L1	14	12
2	L2	10	0
3	L3	91	70
4	L4	66	37
5 ^b	L3	99	83 (69) ^c

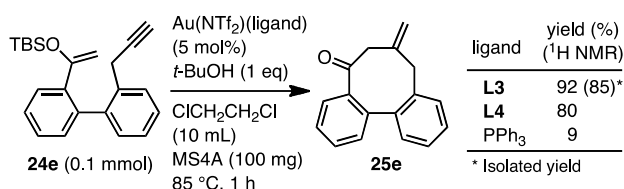
^aDetermined by ¹H NMR spectroscopy. ^bMeOH (0.1 mmol) was used instead of *t*-BuOH. ^cIsolated yield.

Gold catalysts with triarylmethyl-type triethynylphosphine ligands (**L3** and **L4**) were also effective towards the 8-*exo-dig* annulation of monocyclic silyl enol ethers **24b–24d** with different ring sizes in the construction of various bicyclo[5.*n*.1]alkane frameworks **25b–25d** (Scheme 14).

**Scheme 14.** Cyclization of **24b–24d**.

With both **L3** and **L4** as ligands, the cyclization of acetylenic silyl enol ether **24e** with a biphenyl-based rigid

linker occurred smoothly, in affording dibenzocyclooctane derivative **25e** (92% and 80% yields, respectively; Scheme 15). The cyclization of **24e** with a PPh₃-based catalyst gave **25e** in only 9% yield. It is important to note that cyclization product **25e** contains the core structure of the dibenzocyclooctane lignan family of natural products, of which some have been shown to possess important biological properties; in particular, one such compound (Gomisin G, Figure 6) has exhibited potent anti-HIV activity.³⁷



Scheme 15. Cyclization of **24e**.

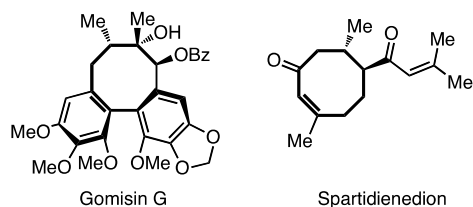


Figure 6. Natural products that possess an eight-membered carbocycle.

Moreover, as shown in Table 10, the gold catalyst with **L4** was also effective towards the 8-*exo-dig* cyclization of acyclic substrates to afford non-fused methylenecyclooctane derivatives. The reaction of substrate **24f**, which possess an unbranched linker between the siloxyalkene and acetylene moieties, afforded 2-acylmethylenecyclooctane **25f**, albeit in yields of merely 23%. The low cyclization efficacy can be attributable to the flexibility of the unbranched substrate. More efficient cyclization occurred in the reaction of the siloxyalkene with a dimethyl malonate insert at the homoallylic position (**24g**), improving the yield to 59% (entry 2). The structure of **25g** was confirmed by a single-crystal X-ray diffraction study (Figure 7).¹⁰ The higher cyclization efficacy for the formation of **25g** than that of **25f** can be attributed to the Thorpe–Ingold effect. In the case of benzyl-substituted terminal siloxyalkene with substituents on the aromatic ring **24h–24l**, the reactions proceeded smoothly to form methylenecyclooctane derivative **25h–25l**, which possesses an endocyclic carbonyl group, and is structurally related to spartidienedione (Figure 6).³⁸ Silyl enol ether **24m**, which possesses two terminal alkyne moieties, was also converted to the monocyclic compound **25m**.

Table 10. Cyclization of Linear Alkynyl Silyl Enol Ethers **24**.^a

entry	substrate 24	product 25	yield (%) ^b
1 ^c			23
2 ^c			59
3			50
4	24i (R = 4-OMe)	25i (R = 4-OMe)	47
5	24j (R = 4-Br)	25j (R = 4-Br)	36
6	24k (R = 2-Br)	25k (R = 2-Br)	42
7	24l (R = 2-I)	25l (R = 2-I)	43
8			66

^a**24** (E = CO₂Me, 0.1 mmol), [Au(NTf₂)(**L4**)] (5 mol%), *t*-BuOH (0.1 mmol), MS4A (100 mg), ClCH₂CH₂Cl (10 mL) at 85 °C, 1 h. ^bIsolated yield. ^cIsomeric mixture for **24f**, *E/Z* 20:80; **24g**, *E/Z* 23:77.

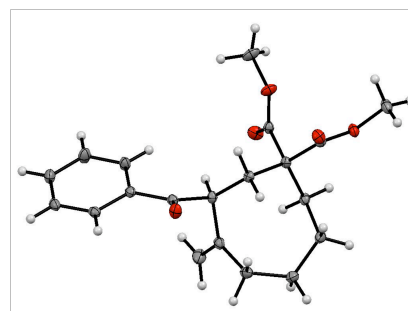
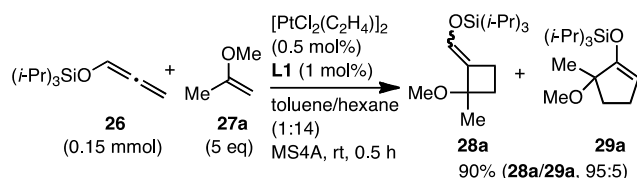


Figure 7. ORTEP drawing of the molecular structure of **25g**.

Platinum(II)-Catalyzed [2+2] Cycloaddition of an Allenyl Silyl Ether with Vinyl Ethers

Iwasawa and coworkers used the hollow-shaped triethynylphosphine **L1** as a ligand for a platinum(II) catalyst in the study of cycloaddition reactions between an allenyl silyl ether (**26**) and vinyl ethers (**27**) (Scheme 16).³⁹ This is the first demonstration of the utility of the hollow-shaped triethynyl phosphines for platinum catalysis. The authors found that **L1** gave active Pt(II) catalyst and showed excellent chemoselectivities giving a [2+2] cycloaddition product (methylenecyclobutane **28**) over a [3+2] cycloaddition product

(cyclopentene **29**) (**28a/29a** 95:5).^{40,41} Pt(II) catalysts prepared from conventional phosphorus ligands such as PPh₃, P(*o*-tol)₃, P(2-furyl)₃, and P(OEt)₃ showed lower chemoselectivities (**28a/29a**, <64:36). Specifically, the reaction of **26** and **27a** with toluene-hexane (1:14) solution of 0.5 mol% of [PtCl₂(C₂H₄)₂] and 1 mol% of **L1** provided a mixture of methylenecyclobutane **28a** and cyclopentene **29a** in the total yield of 90% in a ratio of 95:5 (Scheme 16).

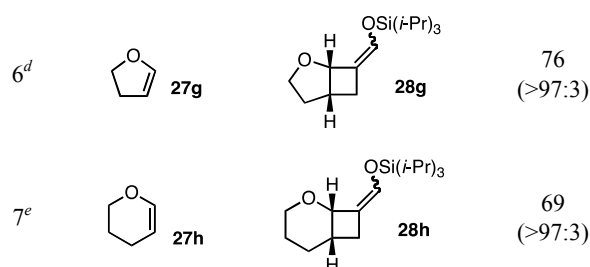


Scheme 16. [2+2] Cycloaddition of **26** and **27a**.

The scope of vinyl ethers **27** for the [2+2] cycloaddition reaction with **26** using the platinum(II)-triethylphosphine (**L1**) catalyst system was shown in Table 11. The reactions of 1,1-disubstituted alkenyl ethers **27b–27d** proceeded smoothly to afford cyclobutanes **28b–28d** in high yields with excellent chemoselectivities (**28/29**, >96:4 in entries 1–3). This protocol was also applicable to cyclic alkenyl ethers **27e–27h**, and the corresponding bicyclic cyclobutanes **28e–28h** were obtained in high selectivities (entries 4–7).

Table 11. [2+2] Cycloaddition Reactions with Various **27**.^a

entry	vinyl ether 27	major product 28	total yield (%) (28/29) ^b
1			86 (>97:3)
2			94 (96:4)
3 ^c			77 (>97:3)
4			98 (94:6)
5			99 (>97:3)



^a**26** (0.15 mmol), **27** (1.1 eq for entries 1–5; 5 eq for entries 6 and 7), [PtCl₂(C₂H₄)₂] (0.5 mol%), **L1** (1 mol%), MS4A (ca. 250 mg), toluene/hexane (1:14, 1.5 mL), rt, 3 h. ^bThe ratio was determined by ¹H NMR analysis. ^cToluene/hexane 1:6.5. ^dFor 16 h. ^eFor 24 h.

Summary

Triethylphosphines (**L1–L4**) with bulky end caps such as triarylsilyl and triarylmethyl groups at alkyne termini are vacant in the vicinity of the phosphorus atom but sterically demanding in the distal region, resulting in the creation of large-scale cavity above the phosphine lone pair. The usefulness as a ligand for transition metal catalysis was demonstrated by the rate enhancement in the rhodium-catalyzed hydrosilylation of ketones, and gold-catalyzed six- to eight-membered ring forming cyclizations of acetylenic keto esters, 1,7-enynes, alkynic sulfonamides, hydroxy-tethered propargylic esters, and acetylenic silyl enol ethers. In the studies of eight-membered carbocycle formation from acetylene-tethered silyl enol ethers, triarylmethyl-type ligands (**L3** and **L4**) gave better product yields than the triarylsilyl-type ligands (**L1** and **L2**). However, the superiority of **L3** and **L4** over **L1** and **L2** has not been demonstrated in general for other reactions. In addition, **L1** was used for platinum-catalyzed [2+2] cycloaddition reaction of an allenyl silyl enol ether with vinyl ethers, resulting in the selective formation of methylenecyclobutanes. Accordingly, the hollow-shaped triethylphosphines are easy to synthesize and handle, and are useful items for the toolbox in catalytic organometallic chemistry.

The authors appreciate intellectual and experimental contributions by our co-workers, Dr. Atsuko Ochida, Dr. Hideto Ito, Dr. Yusuke Makida, Mr. Tomoya Harada, Ms. Ayumi Harada, Ms. Hiori Okochi, and Prof. Hirohisa Ohmiya.

References and Abbreviations

- 1 *Homogeneous Catalysis with Metal Phosphine Complexes*; ed by L. H. Pignolet, Plenum, New York, (1983).
- 2 For the coordination of alkynyl phosphines through the phosphorus atom to a metal center, see: a) J. T. Mague, J. P. Mitchener, *Inorg. Chem.* **1969**, *8*, 119–125. b) E. Louattani, A. Lledós, J. Suades, A. Alvarez-Larena, J. F. Piniella, *Organometallics* **1995**, *14*, 1053–1060. c) M. Bardaji, M. T. de la Cruz, P. G. Jones, A. Laguna, J. Martínez, M. D. Villacampa, *Inorg. Chim. Acta* **2005**, *358*, 1365–1372.
- 3 For multinuclear complexes, see: a) I. Ara, L. R.

Falvello, S. Fernández, J. Forniés, E. Lalinde, A. Martín, M. T. Moreno, *Organometallics* **1997**, *16*, 5923–5937. b) J. R. Berenguer, M. Bernechea, J. Forniés, J. Gómez, E. Lalinde, *Organometallics* **2002**, *21*, 2314–2324.

4 For η^2 -phosphinoalkyne–metal complexes, see: a) M. A. Bennett, J. Castro, A. J. Edwards, M. R. Kopp, E. Wenger, A. C. Willis, *Organometallics* **2001**, *20*, 980–989. b) K. Okamoto, Y. Omoto, H. Sano, K. Ohe, *Dalton Trans.* **2012**, *41*, 10926–10929.

5 For the reactivity of alkynylphosphines, see: a) G. Borkent, W. Drenth, *Recueil. Trav. Chim.* **1970**, *89*, 1057–1067. b) A. J. Carty, S. E. Jacobson, R. T. Simpson, N. J. Taylor, *J. Am. Chem. Soc.* **1975**, *97*, 7254–7262. c) G. Märkl, H. Baier, R. Liebl, *Synthesis* **1977**, 842–845. d) D. K. Johnson, T. Rukachaisirikul, Y. Sun, N. J. Taylor, A. J. Carty, A. J. Carty, *Inorg. Chem.* **1993**, *32*, 5544–5552. e) X. Liu, T. K. W. Ong, S. Selvaratnam, J. J. Vittal, A. J. P. White, D. J. Williams, P.-H. Leung, *J. Organomet. Chem.* **2002**, *643–644*, 4–11.

6 A. Ochida, H. Ito, M. Sawamura, *J. Am. Chem. Soc.* **2006**, *128*, 16486–16487.

7 A. Ochida, M. Sawamura, *Chem. Asian J.* **2007**, *2*, 609–618.

8 T. Iwai, H. Okochi, H. Ito, M. Sawamura, *Angew. Chem. Int. Ed.* **2013**, *52*, 4239–4242.

9 V. V. Afanasiev, I. P. Beletskaya, M. A. Kazankova, I. V. Efimova, M. U. Antipin, *Synthesis* **2003**, 2835–3838.

10 The crystallographic data for **L2** (CCDC-637031), [RhCl(cod)(**L2**)] (CCDC-637032), **22k** (CCDC-787890) and **25g** (CCDC-1009905) can be obtained free of charge from the Cambridge Crystallographic Data Centre at http://www.ccdc.cam.ac.uk/data_request/cif.

11 a) T. Matsumoto, T. Kasai, K. Tatsumi, *Chem. Lett.* **2002**, *31*, 346–347. b) K. Goto, Y. Ohzu, H. Sato, T. Kawashima, *Phosphorus Sulfur Silicon Relat. Elem.* **2002**, *177*, 2179–2180. c) Y. Ohzu, K. Goto, T. Kawashima, *Angew. Chem. Int. Ed.* **2003**, *42*, 5714–5716.

12 a) O. Niyomura, M. Tokunaga, Y. Obora, T. Iwasawa, Y. Tsuji, *Angew. Chem. Int. Ed.* **2003**, *42*, 1287–1289. b) O. Niyomura, T. Iwasawa, N. Sawada, M. Tokunaga, Y. Obora, Y. Tsuji, *Organometallics* **2005**, *24*, 3468–3475.

13 H. Ito, T. Kato, M. Sawamura, *Chem. Lett.* **2006**, *35*, 1038–1039.

14 a) G. Hamasaka, A. Ochida, K. Hara, M. Sawamura, *Angew. Chem. Int. Ed.* **2007**, *46*, 5381–5383. b) G. Hamasaka, S. Kawamorita, A. Ochida, R. Akiyama, K. Hara, A. Fukuoka, K. Asakura, W. J. Chun, H. Ohmiya, M. Sawamura, *Organometallics* **2008**, *27*, 6495–6506.

15 For selected reviews on gold catalysis, see: a) A. Fürstner, P. W. Davies, *Angew. Chem. Int. Ed.* **2007**, *46*, 3410–3349. b) A. S. K. Hashmi, *Chem. Rev.* **2007**, *107*, 3180–3211. c) Z. Li, C. Brouwer, C. He, *Chem. Rev.* **2008**, *108*, 3239–3265. d) A. Arcadi, *Chem. Rev.* **2008**, *108*, 3266–3325. e) D. J. Gorin, B. D. Sherry, F. D. Toste, *Chem. Rev.* **2008**, *108*, 3351–3378. f) A. Corma, A. Leyva-Pérez, M. J. Sabater, *Chem. Rev.* **2011**, *111*, 1657–1712. g) N. Krause, C. Winter, *Chem. Rev.* **2011**, *111*, 1994–2009. h) H. Huang, Y. Zhou, H. Liu, *Beilstein J. Org. Chem.* **2011**, *7*, 897–936. i) B.-L. Lu, L. Dai, M. Shi, *Chem. Soc. Rev.* **2012**, *41*, 3318–3339. j) L.-P. Liu, G. B. Hammond, *Chem. Soc. Rev.* **2012**, *41*, 3129–3139.

16 J. M. Conia, P. Le Perchec, *Synthesis* **1975**, 1–19.

17 For selected examples of the gold-catalyzed Conia-ene reactions, see: a) J. J. Kennedy-Smith, S. T. Staben, F. D. Toste, *J. Am. Chem. Soc.* **2004**, *126*, 4526–4527. b) S. T. Staben, J. J. Kennedy-Smith, F. D. Toste, *Angew. Chem. Int. Ed.* **2004**, *43*, 5350–5352. c) N. Mézailles, L. Ricard, F. Gagosz, *Org. Lett.* **2005**, *7*, 4133–4136.

18 Selected examples of Conia-ene reactions catalyzed by other metals. For Co: a) P. Cruciani, R. Stammer, C. Aubert, M. Malacria, *J. Org. Chem.* **1996**, *61*, 2699–2708. For Mo: b) F. E. McDonald, T. C. Olson, *Tetrahedron Lett.* **1997**, *38*, 7691–7692. For Zn: c) E. Nakamura, G. Sakata, K. Kubota, *Tetrahedron Lett.* **1998**, *39*, 2157–2158. For Ti: d) O. Kitagawa, T. Suzuki, T. Inoue, Y. Watanabe, T. Taguchi, *J. Org. Chem.* **1998**, *63*, 9470–9475. For Cu: e) D. Bouyssi, N. Monteiro, G. Balme, *Tetrahedron Lett.* **1999**, *40*, 1297–1300. For Sn: f) O. Kitagawa, H. Fujiwara, T. Suzuki, T. Taguchi, M. Shiro, *J. Org. Chem.* **2000**, *65*, 6819–6825. For Ni: g) Q. Gao, B.-F. Zheng, J.-H. Li, D. Yang, *Org. Lett.* **2005**, *7*, 2185–2188. For Re: h) Y. Kuninobu, A. Kawata, K. Takai, *Org. Lett.*, **2005**, *7*, 4823–4825. For Pd: g) B. K. Corkey, F. D. Toste, *J. Am. Chem. Soc.*, **2005**, *127*, 17168–17169. For In: h) H. Tsuji, K.-i. Yamagata, Y. Itoh, K. Endo, M. Nakamura, E. Nakamura, *Angew. Chem. Int. Ed.* **2007**, *46*, 8060–8062. For Fe: i) L. Y. Chan, S. Kim, Y. Park, P. H. Lee, *J. Org. Chem.* **2012**, *77*, 5239–5244.

19 R. Martin, S. L. Buchwald, *Acc. Chem. Res.* **2008**, *41*, 1461–1473.

20 H. Ito, Y. Makida, A. Ochida, H. Ohmiya, M. Sawamura, *Org. Lett.* **2008**, *10*, 5051–5054.

21 C. Nieto-Oberhuber, M. P. Muñoz, E. Buñuel, C. Nevado, D. J. Cárdenas, A. M. Echavarren, *Angew. Chem. Int. Ed.* **2004**, *43*, 2402–2406.

22 For selected reviews on metal-catalyzed cycloisomerizations, see: a) C. Aubert, O. Buisine, M. Malacria, *Chem. Rev.* **2002**, *102*, 813–834. b) G. C. Lloyd-Jones, *Org. Biomol. Chem.* **2003**, *1*, 215–236. c) S. T. Diver, A. J. Giessert, *Chem. Rev.* **2004**, *104*, 1317–1382. d) L. Zhang, J. Sun, S. A. Kozmin, *Adv. Synth. Catal.* **2006**, *348*, 2271–2296. e) E. Jiménez-Núñez, A. M. Echavarren, *Chem. Rev.* **2008**, *108*, 3326–3350. f) V. Michelet, P. Y. Toullec, J.-P. Genêt, *Angew. Chem. Int. Ed.* **2008**, *47*, 4268–4315. g) C. Aubert, L. Fensterbank, P. Garcia, M. Malacria, A. Simonneau, *Chem. Rev.* **2011**, *111*, 1954–1993.

23 a) R. A. Pilli, M. C. Ferreira de Oliveira, *Nat. Prod. Rep.* **2000**, *17*, 117–127. b) R. Alibés, M. Figueredo, *Eur. J. Org. Chem.* **2009**, 2421–2435. c) S. M. Weinreb, M. F. Semmelhack, *Acc. Chem. Res.* **1975**, *8*, 158–164.

24 For selected reviews, see: a) T. E. Müller, M. Beller, *Chem. Rev.* **1998**, *98*, 675–704. b) T. E. Müller, K. C. Hultsch, M. Yus, F. Foubelo, M. Tada, *Chem. Rev.* **2008**, *108*, 3795–3892. c) A. Corma, A. Leyva-Pérez, M. J. Sabater, *Chem. Rev.* **2011**, *111*, 1657–1712.

25 H. Ito, T. Harada, H. Ohmiya, M. Sawamura, *Beilstein J. Org. Chem.* **2011**, *7*, 951–959.

26 G. C. Fortman, S. P. Nolan, *Chem. Soc. Rev.* **2011**, *40*, 5151–5169.

27 H. Ito, A. Harada, H. Ohmiya, M. Sawamura, *Adv. Synth. Catal.* **2013**, *355*, 647–652.

28 a) J. K. De Brabander, B. Liu, M. Qian, *Org. Lett.* **2008**, *10*, 2533–2536. b) Q. Liang, J. K. De Brabander,

Tetrahedron **2011**, *67*, 5046–5053. c) Y.-M. Wang, C. N. Kuzniewski, V. Rauniyar, C. Hoong, F. D. Toste, *J. Am. Chem. Soc.* **2011**, *133*, 12972–12975. d) J. Huang, X. Huang, B. Liu, *Org. Biomol. Chem.* **2010**, *8*, 2697–2699.

29 Selected examples of rearrangement of propargyl esters catalyzed by metals other than gold. For Zn: a) H. Strickler, J. B. Davis, G. Ohloff, *Helv. Chim. Acta* **1976**, *59*, 1328–1332. For Pd: b) V. Rautenstrauch, *J. Org. Chem.* **1984**, *49*, 950–952. For Pt: c) E. Mainetti, V. Mouriès, L. Fensterbank, M. Malacria, J. Marco-Contelles, *Angew. Chem. Int. Ed.* **2002**, *41*, 2132–2135. For Ru: d) K. Miki, K. Ohe, S. Uemura, *Tetrahedron Lett.* **2003**, *44*, 2019–2022.

30 For selected reviews on metal-catalyzed rearrangement of propargyl esters, see: a) N. Marion, S. P. Nolan, *Angew. Chem. Int. Ed.* **2007**, *46*, 2750–2752. b) J. Marco-Contelles, E. Soriano, *Chem. Eur. J.* **2007**, *13*, 1350–1357. c) S. Wang, G. Zhang, L. Zhang, *Synlett* **2010**, 692–706.

31 For selected examples of gold catalysis, see: a) S. T. Stuben, J. J. Kennedy-Smith, D. Huang, B. K. Corkey, R. L. LaLonde, F. D. Toste, *Angew. Chem. Int. Ed.* **2006**, *45*, 5991–5994. b) K. Lee, P. H. Lee, *Adv. Synth. Catal.* **2007**, *349*, 2092–2096. c) E. C. Minnihan, S. L. Colletti, F. D. Toste, H. C. Shen, *J. Org. Chem.* **2007**, *72*, 6287–6289. d) F. Barabé, G. Bétournay, G. Bellavance, L. Barriault, *Org. Lett.* **2009**, *11*, 4236–4238. e) H. Kusama, Y. Karibe, Y. Onizawa, N. Iwasawa, *Angew. Chem. Int. Ed.* **2010**, *49*, 4269–4272. f) F. Barabé, P. Levesque, I. Korobkov, L. Barriault, *Org. Lett.* **2011**, *13*, 5580–5583. g) B. Sow, G. Bellavance, F. Barabé, L. Barriault, *Beilstein J. Org. Chem.* **2011**, *7*, 1007–1013. h) J.-F. Brazeau, S. Zhang, I. Colomer, B. K. Corkey, F. D. Toste, *J. Am. Chem. Soc.* **2012**, *134*, 2742–2749.

32 Selected examples of other metal catalysis. For Hg: a) J. Drouin, M.-A. Boaventura, J.-M. Conia, *J. Am. Chem. Soc.* **1985**, *107*, 1726–1729. For Al: b) K.-i. Imamura, E. Yoshikawa, V. Gevorgyan, Y. Yamamoto, *Tetrahedron Lett.* **1999**, *40*, 4081–4084. For W: c) K. Maeyama, N. Iwasawa, *J. Am. Chem. Soc.* **1998**, *120*, 1928–1929. For Rh: d) J. W. Dankwardt, *Tetrahedron Lett.* **2001**, *42*, 5809–5812. For Pt: e) C. Nevado, D. J. Cárdenas, A. M. Echavarren, *Chem. Eur. J.* **2003**, *9*, 2627–2635. For Re: f) H. Kusawa, H. Yamabe, Y. Onizawa, T. Hoshino, N. Iwasawa, *Angew. Chem. Int. Ed.* **2005**, *44*, 468–470. g) For Pd: B. K. Corkey, F. D. Toste, *J. Am. Chem. Soc.* **2007**, *129*, 2764–2765. For Ag: h) T. Godet, P. Belmont, *Synlett* **2008**, 2513–2517.

33 H. Ito, H. Ohmiya, M. Sawamura, *Org. Lett.* **2010**, *12*, 4380–4383.

34 a) M. Ishitsuka, T. Kusumi, H. Kakisawa, *Tetrahedron Lett.* **1982**, *23*, 3179–3180. b) M. P. Kirkup, R. E. Moore, *Phytochemistry* **1983**, *22*, 2527–2529.

35 B. Esquivel, J. Cárdenas, A. Toscano, M. Soriano-García, L. Rodríguez-Hahn, *Tetrahedron* **1985**, *41*, 3213–3217.

36 M. M. Pandey, S. Rastogi, A. K. S. Rawat, *J. Ethnopharmacol.* **2007**, *110*, 379–390.

37 D.-F. Chen, S.-X. Zhang, L. Xie, J.-X. Xie, K. Chen, Y. Kashiwada, B.-N. Zhou, P. Wang, L. M. Cosentino, K.-H. Lee, *Bioorg. Med. Chem.* **1997**, *5*, 1715–1723.

38 M. Norte, F. Cataldo, A. Sánchez, A. G. González, P. Rivera, M. Castillo, *Tetrahedron Lett.* **1993**, *34*, 5143–5146.

39 M. Ebisawa, H. Kusama, N. Iwasawa, *Chem. Lett.*

2012, *41*, 786–788.

40 For selected reviews on cycloadditions of allenes, see: a) S. Ma, *Chem. Rev.* **2005**, *105*, 2829–2872. b) B. Alcaide, P. Almendros, C. Aragoncillo, *Chem. Soc. Rev.* **2010**, *39*, 783–816.

41 H. Kusama, M. Ebisawa, H. Funami, N. Iwasawa, *J. Am. Chem. Soc.* **2009**, *131*, 16352–16353.

Transition Metal Catalysis with Hollow-shaped Triethynylphosphine Ligands

T. Iwai, and M. Sawamura

